11th ANKARA INTERNATIONAL AEROSPACE CONFERENCE **AIAC-2021-088**
8-10 September 2021 - METU, Ankara TURKEY

# GRID FIN AERODYNAMIC ANALYSIS AND PARAMETRIC DESIGN STUDY IN SUPERSONIC FLOW USING COMPUTATIONAL FLUID DYNAMICS

Erdem DİNÇER[1]
Middle East Technical University
Roketsan Missiles Inc.
Ankara, Turkey

Nilay SEZER UZOL[2]
Middle East Technical University
Ankara, Turkey

## ABSTRACT

*Modern tactical missiles became more maneuverable and faster recently. Designing such missiles requires highly efficient control surfaces. Grid fins are unconventional control surfaces, formed by small intersecting planar surfaces supported by an outer frame, which endures challenging flight conditions. In this paper, MICOM Grid Fin [Miller, 1994] wind tunnel experiments are used as a test case to validate the grid fin CFD analysis with polyhedral mesh elements. Several grid fin geometries are investigated in Mach number of 2.5 and four different angles of attack between 0° and 15°. Geometric design parameters are chosen as the gap between members, the web profile angle and the web leading and trailing wedge lengths, and a design study is performed.*

## INTRODUCTION

Aerodynamic control surfaces are vital components for any aerial vehicle to make pitch, yaw, and roll maneuvers to change attitude of aircrafts. For a missile, a control surface consists of fins that can be deflected back and forth to generate forces and moments. Grid fin, also known as lattice fin, is an unconventional form of tail control which is formed by small intersecting planar surfaces supported by an outer frame. Unlike conventional fins, grid fins are mounted perpendicular to the flow allowing the incoming air to pass through.

In highly agile missiles, such as air to air missiles, the control surfaces are exposed to enormous forces and moments during its flight, therefore, lower hinge moment production is always favorable. Main advantage of the grid fin is that grid fins produce very low hinge moments. Due to small chord length, variation in the center of pressure becomes smaller resulting in very small hinge moments. Moreover, grid fins have superior lifting and stall characteristics which increases the control capability of a missile. In addition to efficient packaging, internal structure provides remarkably high strength-to-weight ratio. The main drawback of grid fin is high drag forces [Theerthamalai, 2006]. Other disadvantage is complexity of the geometry which makes it hard to design and produce such devices. Complexity can also be observed in the flow behavior. In transonic speeds, the flow chocking phenomenon appears and grid fin acts as a single blunt body forming a detached bow shock in front of itself. In low supersonic region shocks are reflected and interact with each other

[1] GRA, Engineer, Email: erdem.dincer@roketsan.com.tr
[2] Assoc. Prof. Dr. in Aerospace Engineering Department, Email: nuzol@metu.edu.tr

inside the grid structure. Even in high supersonic speeds where grid fins are the most favorable, oblique shocks disturb the flow behavior in the downstream [Ravindra, 2009].

Computational Fluid Dynamics (CFD) has been used to simulate flow fields around grid fins and to understand grid fin aerodynamics and flow physics in recent literature. There are several studies, some of which are dedicated to validating computational methods [DeSpirito, 2000], some of them are comparing conventional planar fins and grid fins [Munavar, 2010], and others are investigating the grid fin flow field [Hughson, 2007] using CFD. There are also a few studies about exploring the effects of different parameters on grid fin aerodynamics [Debiasi, 2010], and grid fin optimization studies [Peng, 2018] using CFD.

The purpose of this study is to perform a parametric study on grid fins using CFD and a commercial CFD software, ANSYS Fluent, is used in the analysis. Parameters of interest in this study are the gap between web members, web profile angle and the *web leading and trailing wedge lengths*. Different grid fin geometries are investigated for Mach number of 2.5 and four angles of attack between 0° and 15°.

## METHODOLOGY

### Geometry and Design Parameters and Procedure

Creating grid fin geometries is a difficult task to accomplish because a lot of parameters should be taken into consideration. In this study, only the gap between the web profile and the web profile geometry are changed as design parameters. However, in addition, the frame thickness is set to be twice as thick as the web thickness. Hence, as the web thickness varies with the web profile geometry definition, the frame thickness parameter has been changed implicitly as well. Grid fin parameters are shown in Figure 1.

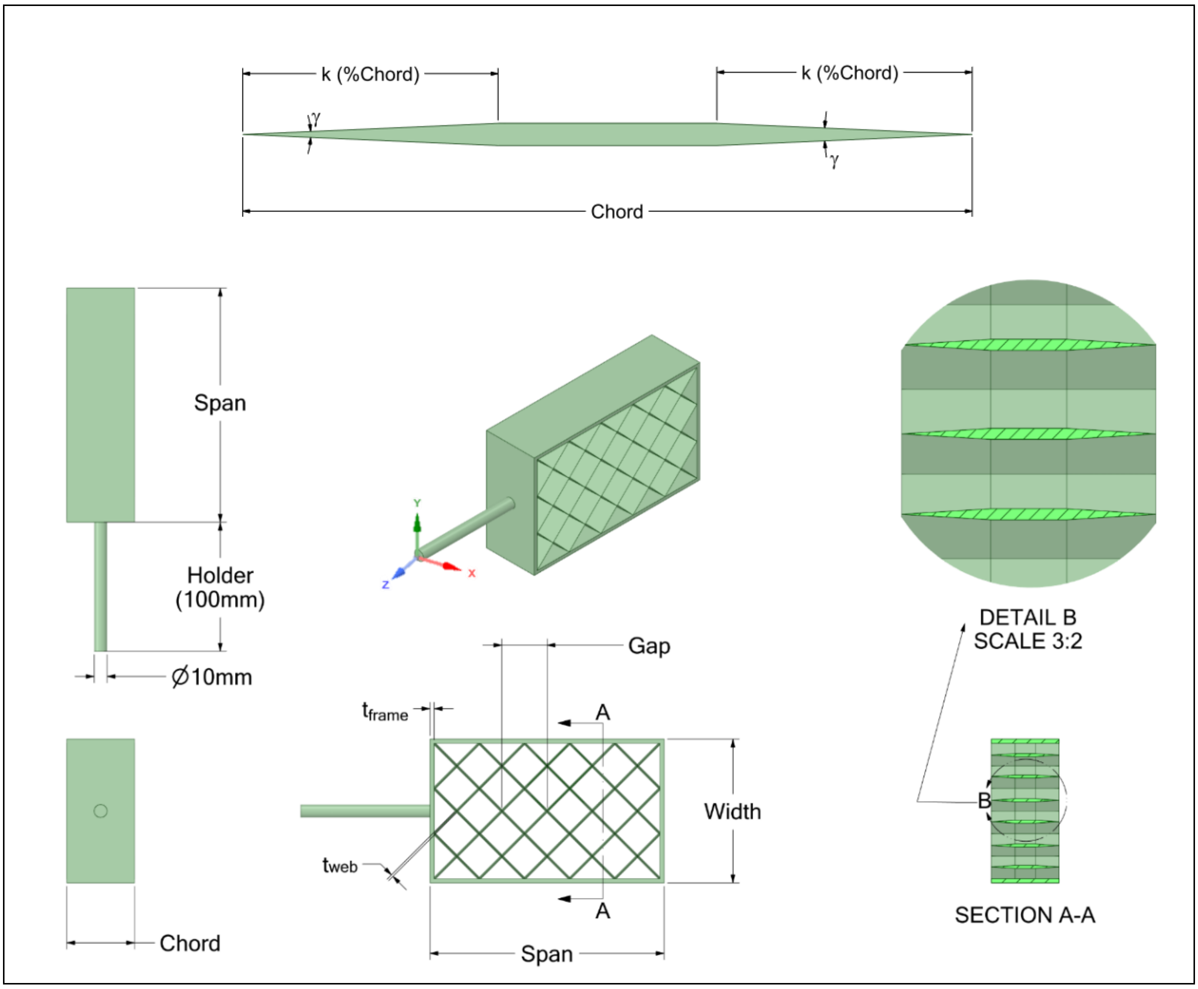


Figure 1: Grid Fin Geometric Parameters

The details of geometries used in the parametric design study is given in Table 1. Each geometry is given a design number and will be mentioned with this number in this paper. In this study, effect of gap between web members, web leading and trailing edge wedge length (*k*) and wedge angle are investigated. First, a baseline design is selected as Design-1 and then three different designs, including Design-1, are compared with respect to each parameter of interest while the rest of the parameters are held constant. Hence, there are total of 7 different design cases for which the detailed CFD simulations are performed.

Table 1: Geometric Parameters of Investigated Designs

| Design # | Gap [mm] | k | ϒ [°] | Wetted Area [$m^2$] | Chord [mm] | Span-Gap Ratio | Width-Gap Ratio |
|---|---|---|---|---|---|---|---|
| 1 | 35 | 0.35 | 5 | 0.2120 | 52.5 | 5 | 3 |
| 2 | 20 | 0.35 | 5 | 0.1183 | 52.5 | 5 | 3 |
| 3 | 50 | 0.35 | 5 | 0.3056 | 52.5 | 5 | 3 |
| 4 | 35 | 0.2 | 5 | 0.2121 | 52.5 | 5 | 3 |
| 5 | 35 | 0.5 | 5 | 0.2134 | 52.5 | 5 | 3 |
| 6 | 35 | 0.35 | 2 | 0.2135 | 52.5 | 5 | 3 |
| 7 | 35 | 0.35 | 8 | 0.2105 | 52.5 | 5 | 3 |

## Computational Approach and CFD Simulation Procedure

In this study, three-dimensional (3-D), steady-state calculations are performed by using the commercial CFD software, ANSYS Fluent Version 20.1. In these numerical calculations, Reynolds-Averaged Navier-Stokes (RANS) equations are solved by using the finite volume method. A modified form of the *k*-ε two-equation turbulence model, which is called "realizable" in Fluent, is used. It differs from the standard *k*-ε model in two important ways: the realizable model contains an alternative formulation for the turbulent viscosity and a modified transport equation for the dissipation rate which was derived from an exact equation for the transport of the mean-square vorticity fluctuation. [ANSYS Fluent Theory Guide]

The geometries are generated using the design modeler, SpaceClaim, which is supplied in Fluent software suite. Grid fin geometries are attached to a symmetry plane with a 100-mm-long cylindrical stick defined as "holder" in Figure 1.

In this study, four different angles of attack from 0° to 15° are investigated at the Mach number of 2.5 in sea level with a 101325 Pa atmospheric pressure and 288 K temperature.

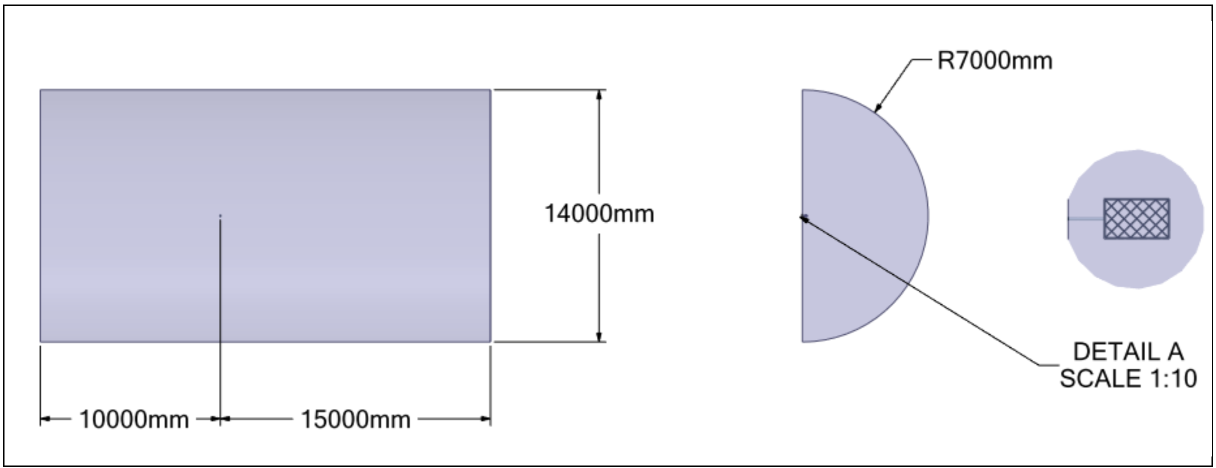


Figure 2*:* Computational Domain: a half cylindrical domain with a single grid fin

Since only a single grid fin geometry is to be solved during the design study because of the computational cost, the computational domain is constructed as a half cylinder containing the geometry. The computational domain details are shown in Figure 2. In this half cylinder enclosure, the surface, where grid fin geometry is attached via the "holder", is defined as the "symmetry" boundary condition in fluent. Basically, this boundary condition satisfies that no flow crosses that boundary, and it is not treated as a wall, therefore no boundary layer grows on this region. For the rest of the enclosure region, a far-field pressure boundary condition is used. Also, a no-slip wall boundary condition is used for all solid regions of the grid fin.

In the unstructured grid generation process, polyhedral cell elements are generated using Fluent Meshing package. The boundary layer mesh spacing is used near the grid fin geometry. In the near-wall region, 20-layers of viscous padding elements are created to obtain a well-captured boundary layer. A systematic grid independence study has not been performed however y+ value is kept smaller than 1.5 with grid clustering around the fin geometry. Since the grid fin geometries are different from each other, the total number of cells are changing between 2.5 million and 8.4 million. A sample mesh distribution is shown in Figure 3 and 4.

In CFD calculations, implicit formulation is used along with $2^{nd}$ Order Upwind discretization and ROE Flux Difference Splitting scheme. The simulations are run with a maximum Courant-Friedrich-Lewy (CFL) number of 7 for these geometries and last about 5000 iterations.

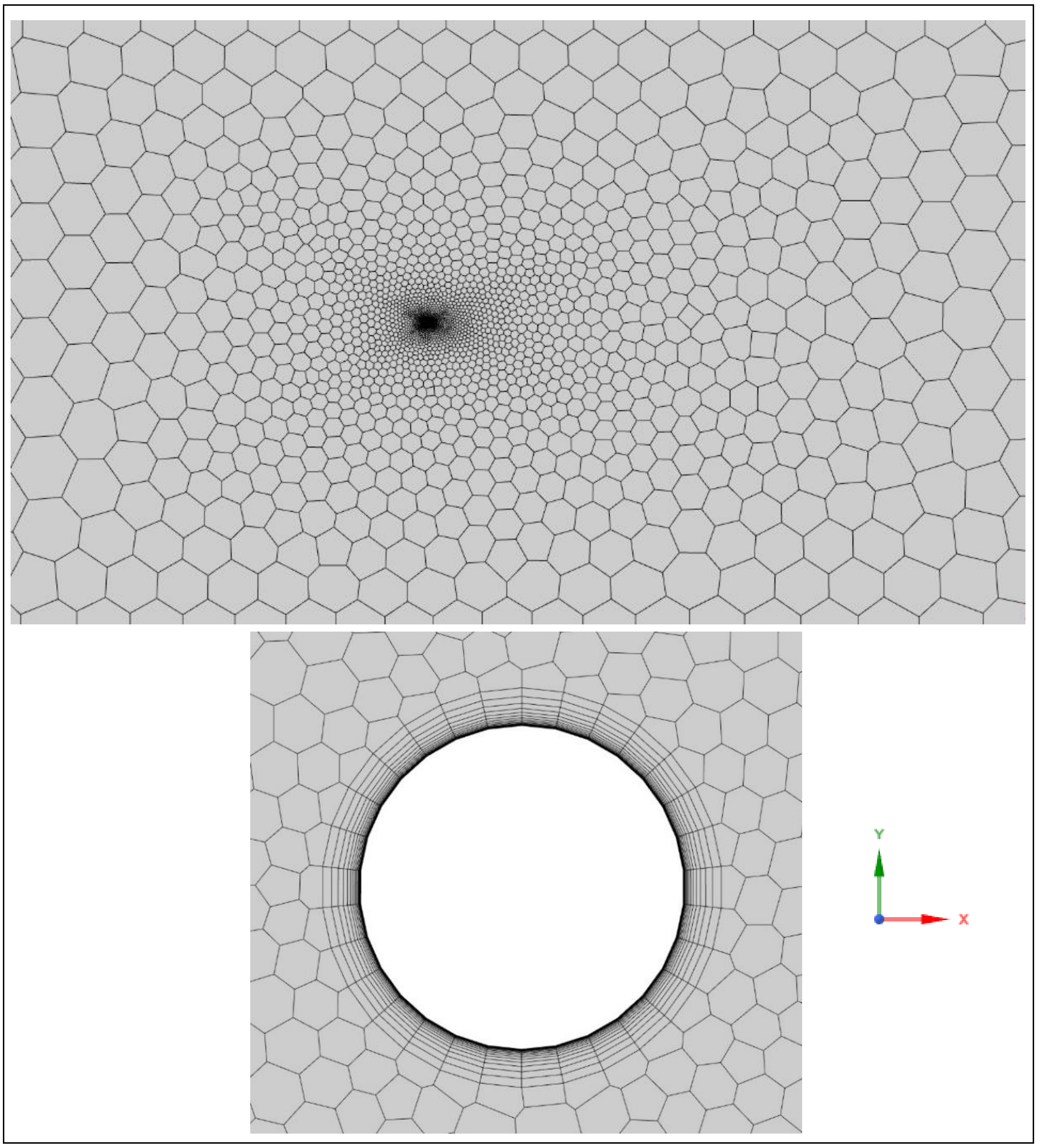


Figure 3: Unstructured Polyhedral Mesh: Symmetry Plane (looking from +z)

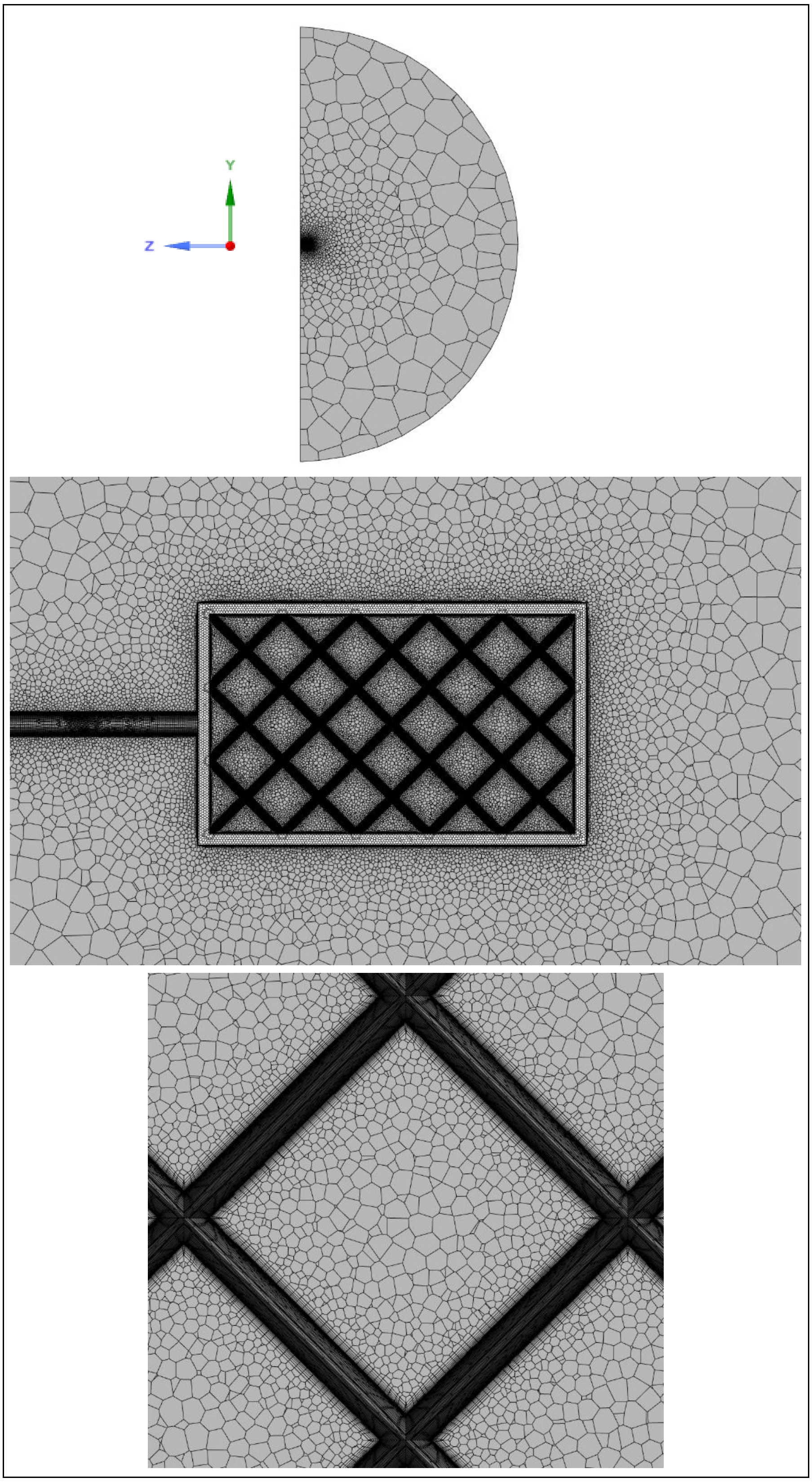


Figure 4*: :* Unstructured Polyhedral Mesh: Cutting the grid fin (looking from +x)

## Validation Test Case for Grid Fin

A validation test case study is carried out for MICOM Grid Fin model, and the results are compared with the available wind tunnel experiments [Miller, 1994]. MICOM grid fin geometry is given in Figure 5. The model is a 52-inch-long, 5-inch diameter body-of-revolution with a 3.0 caliber tangent ogive nose faired into a 7.4 caliber afterbody. Four fins are mounted 2.0 caliber forward of the base. MICOM grid fin placement is shown in Figure 6, where the fins are numbered starting from the top in the clockwise direction. All experimental data presented in this section are obtained from the fin numbered as 4. The sign convention used for the experiments is also given in Figure 6.

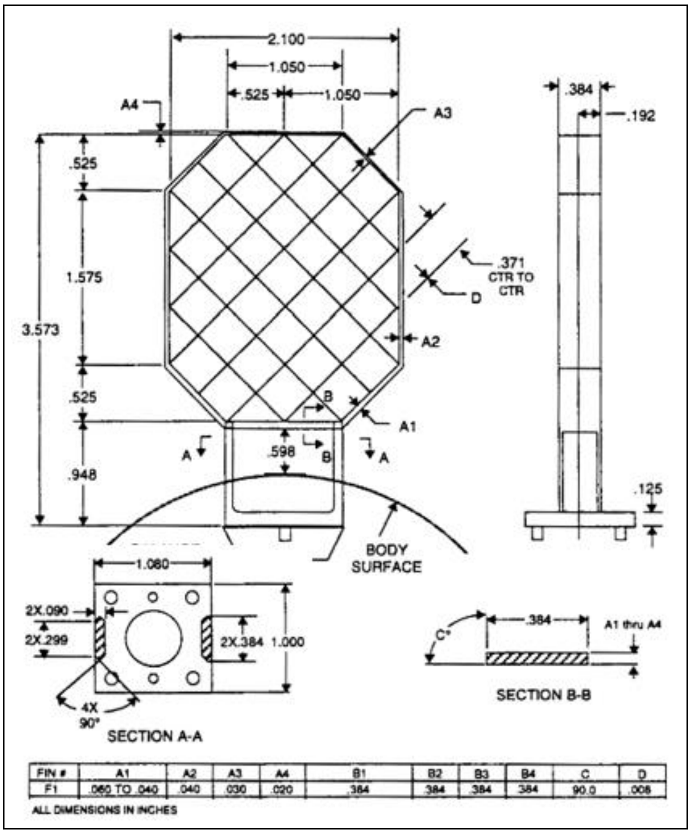


| FIN # | A1 | A2 | A3 | A4 | B1 | B2 | B3 | B4 | C | D |
|---|---|---|---|---|---|---|---|---|---|---|
| F1 | .060 TO .040 | .040 | .030 | .020 | .384 | .384 | .384 | .384 | 90.0 | .008 |

Figure 5*:* MICOM Grid Fin Geometry [Miller, 1994]

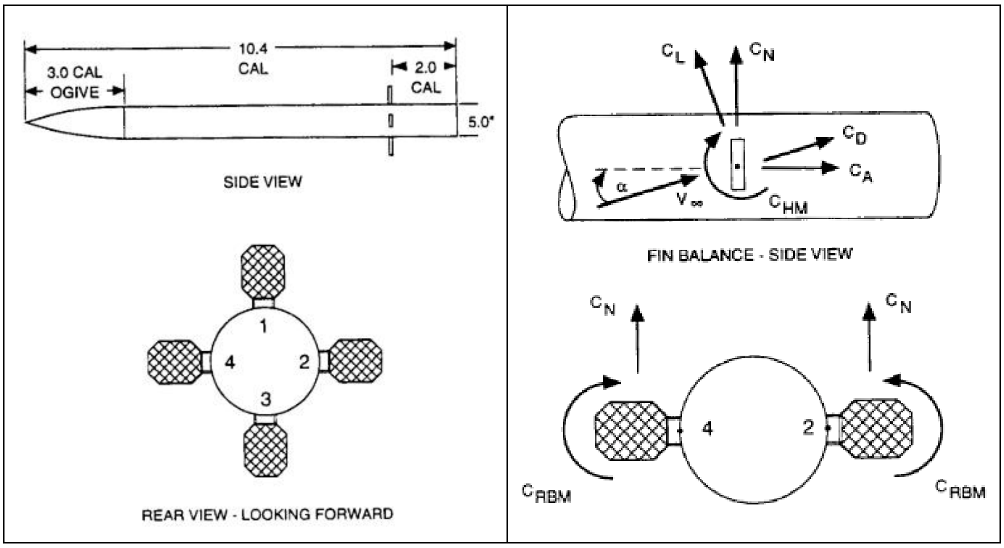


Figure 6*:* Grid Fin Placement and Model Details (left), and Sign Convention (right) [Miller, 1994]

In this validation study, and 2nd order steady state analysis are performed with $k-\varepsilon$ Realizable turbulence model. 6.3 million grid cell elements are used with 20 layers of viscous padding. Due to complex geometry of grid fins, enormous number of mesh elements are required to achieve good mesh resolution. Polyhedral mesh elements can be used to reduce the number of mesh elements and therefore the computational time without loss of accuracy [Rao, 2020]. Therefore, polyhedral mesh elements are used in the validation study and good agreement with the experimental data is achieved as shown in Figure 7 where the computational results are compared with experimental data.

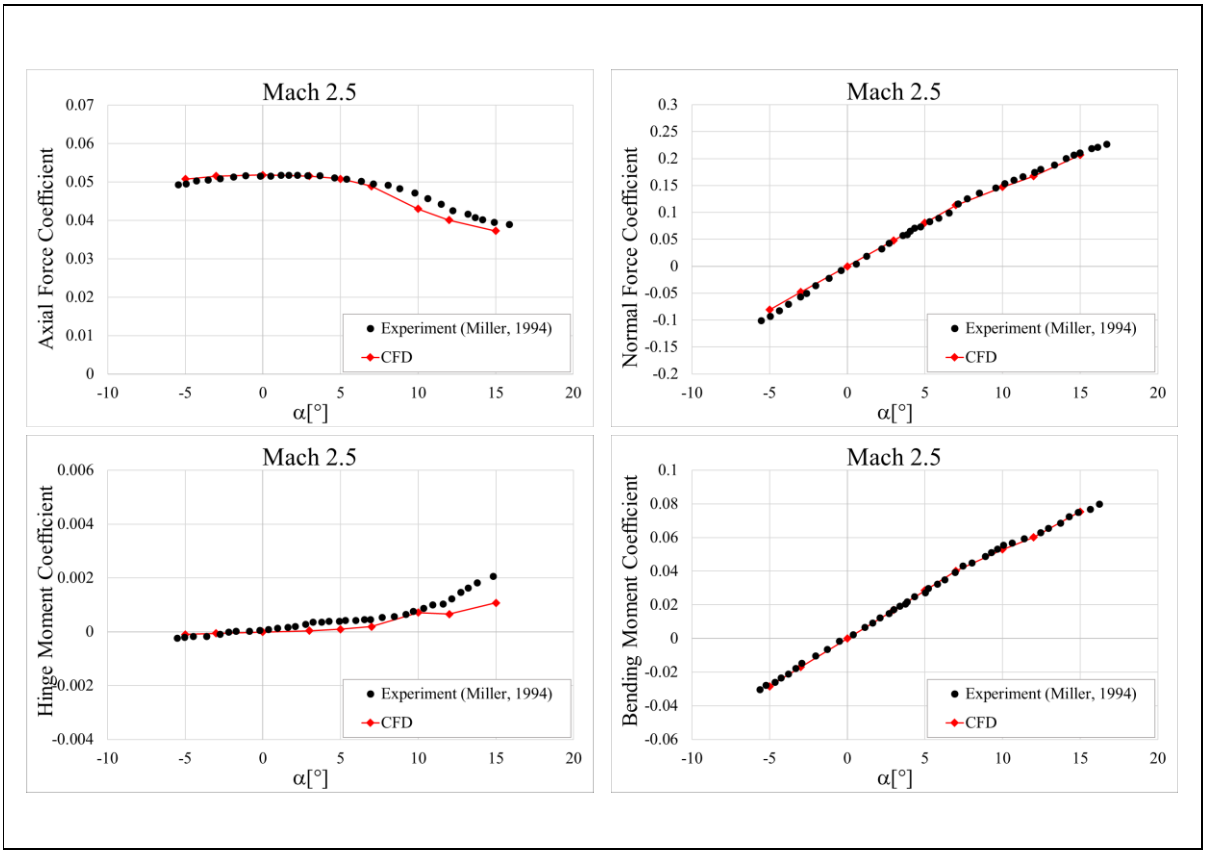


Figure 7: Comparison of the CFD simulations with the experimental data for MICOM Grid Fin model for a range of angle of attack at Mach number of 2.5.

## RESULTS and DISCUSSION

The computational results obtained from the CFD simulations are presented here. The aerodynamic coefficients are non-dimensionalized by using the total wetted area of grid fin for each design since using a constant value for reference area may be misleading for this study. The sign convention is the same with the fin numbered as 2 in Figure 6 in the validation section. In each section the computational results are plotted for each aerodynamic coefficient with respect to parameter of interest including four angles of attack in the same graph. In flow field comparisons, 10° angle of attack is investigated since all aerodynamic coefficients have similar behavior for the range of angle of attacks considered in this study.

### Effects of Gap Between Web Members

In this part, the designs numbered as 1,2 and 3 are used where the gap between the web members are changed between 20 to 50 millimeters. The aerodynamic coefficients obtained from the computational results are shown in Figure 8. Increasing the gap leads to a decrease in the axial force coefficient and an increase in the normal force and bending moment coefficients. In Figure 9, the Mach contours for corresponding designs are shown on a slice cutting the web profiles and showing the flow through the grid fin. When the flow field is investigated, it can be seen that in Design-2 with the smallest gap, the flow chocking phenomenon is observed. The grid fin acts as a single body having a bow shock in the upstream region and this leads to an increase in the axial force coefficient. Also, since there is no pressure difference between upper and lower regions of web members, it results in an excessive loss in the normal force and bending moment coefficients. The axial force coefficient decreases about 44%, the normal force coefficient increases about 62% and the bending moment coefficient increases about 86% between the Design-2 with smallest gap and the Design-3 with the largest gap. The increase in bending moment is also resulting from the increase in the spanwise distance as the gap increased. The bending moment is calculated with respect to the root section of the grid fin where the holder and the grid fin are attached to each other, hence, increasing the span increases the moment arm length and the resulting bending moment.

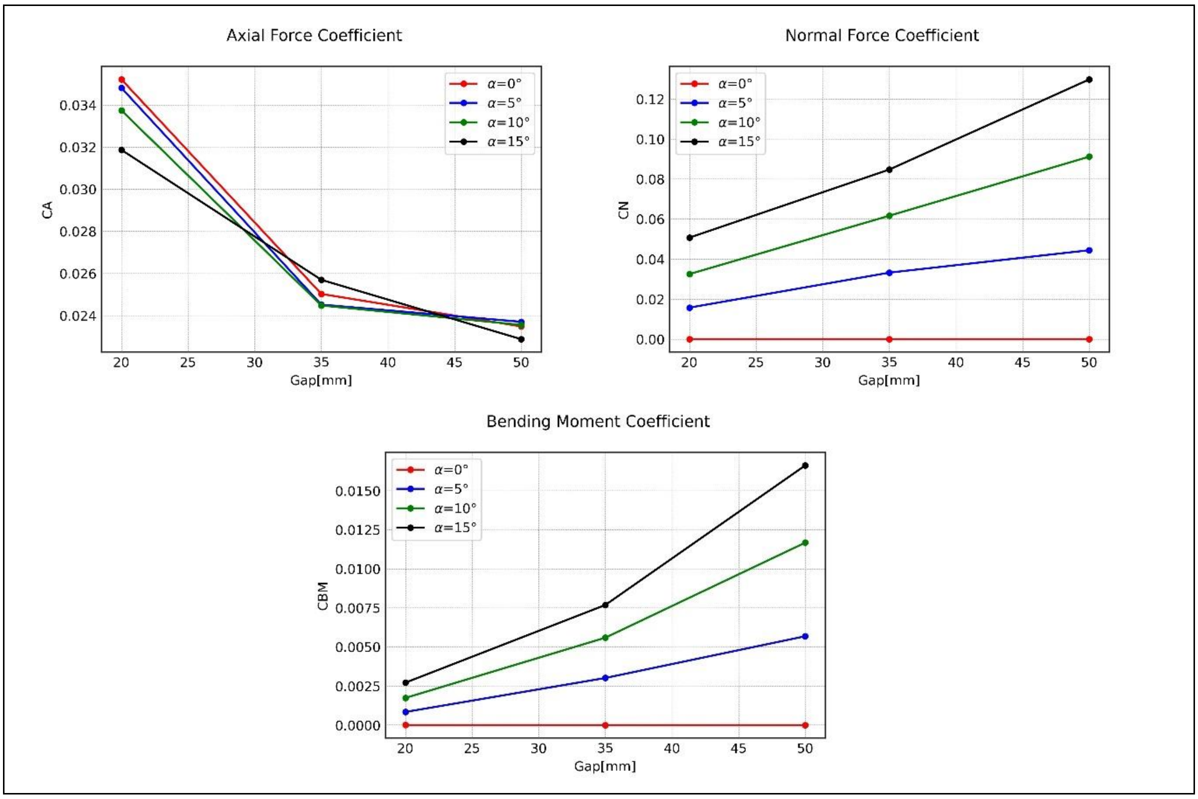


Figure 8: Aerodynamic Coefficients: Axial Force, Normal Force and Bending Moment Coefficients vs Web Gap

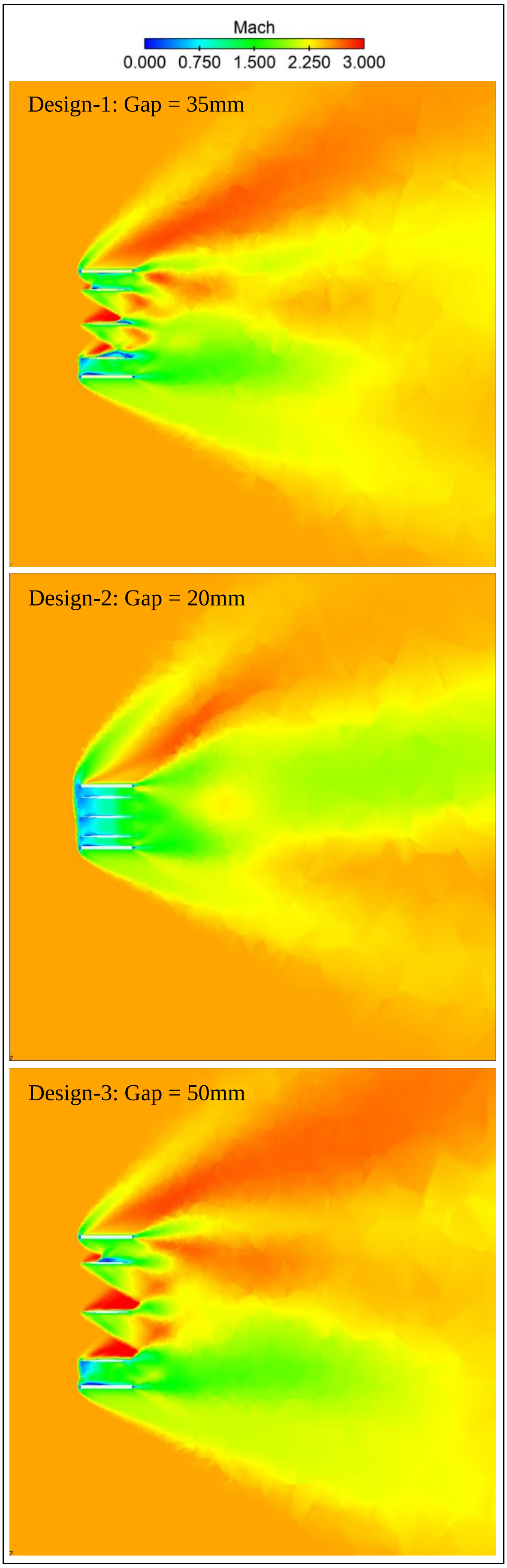


Figure 9: Mach Contours of Designs 1,2 and 3 with different Web Gap

**Effects of Web Member Wedge Length**

In this part, the designs numbered as 1,4 and 5 are used where the wedge lengths are changed. The length of the web profile leading and trailing edge wedge parts are changed between 20 to 50 percent of chord length. When 50 percent wedge length is used, the profile becomes a double-wedge profile. Also, since the wedge angle are kept the same in this part of the study, as the wedge length "*k*" is increased, the web total thickness and consequently the frame thickness are increased as well. This thickness increases should be taken into consideration when interpreting solutions. The aerodynamic coefficients obtained from the computational results are shown in Figure 10. Increasing the wedge length increases the axial force coefficient, however, slightly decreases the normal force and bending moment coefficients. In Figure 11, the Mach contours for corresponding designs are shown on a slice cutting the profiles and showing the flow through the grid fin. When the flow field is investigated, it can be observed that in Design-5 where a double-wedge profile is used with 50% wedge length, the partial flow chocking phenomenon is observed. This flow behavior explains the slight decrease in the normal force and bending moment coefficients. The axial force coefficient of Design-5 is 1.5 times of the Design-4. Also, the web and frame thicknesses of Design-5 are 2.5 times the Design-4.

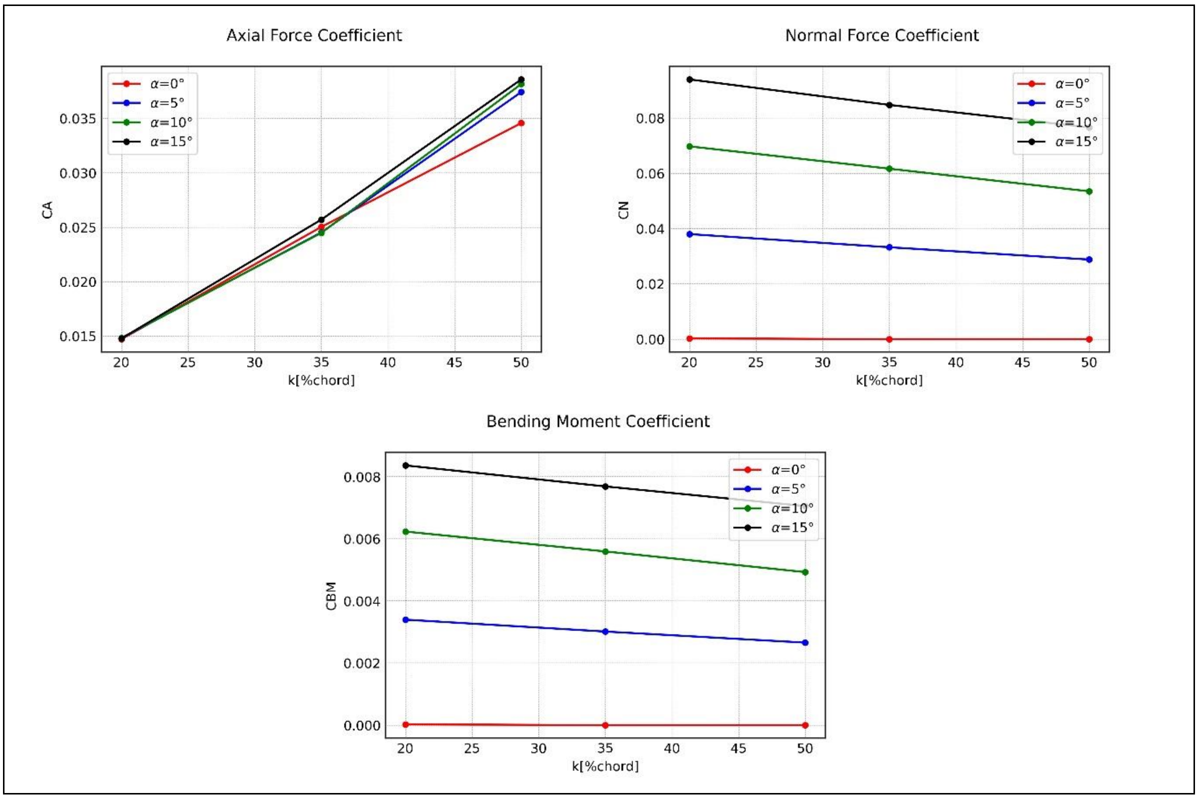


Figure 10*:* Aerodynamic Coefficients: Axial Force, Normal Force and Bending Moment Coefficients vs Web Members Wedge Length (*k*)

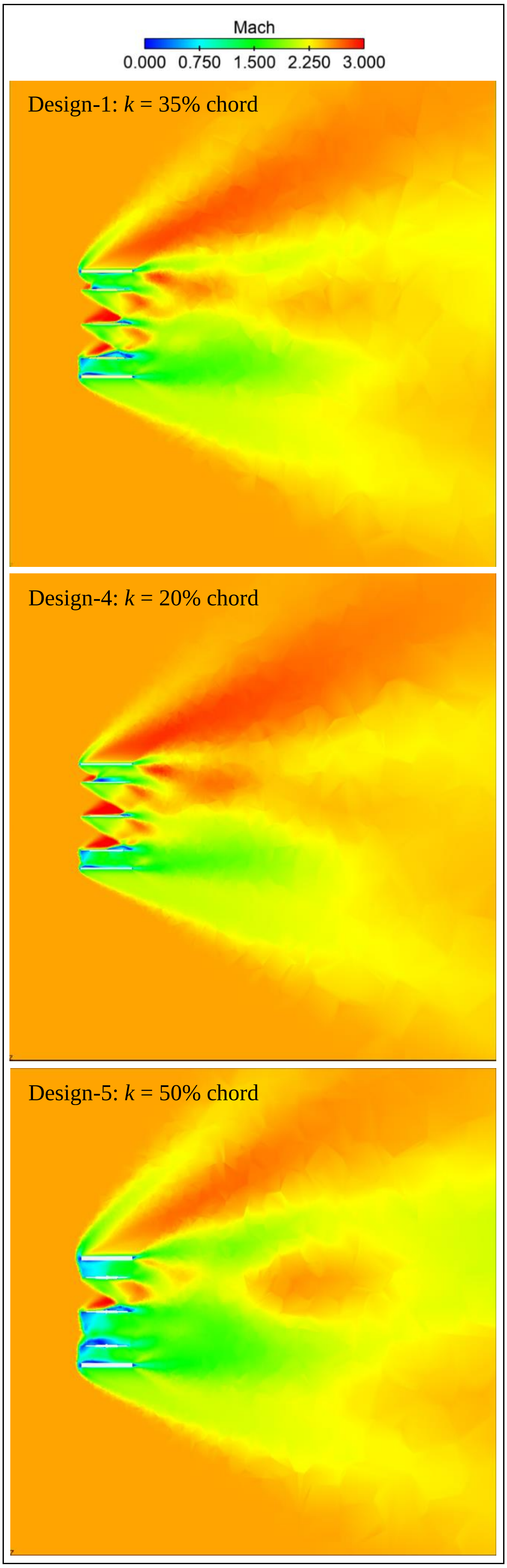


Figure 11*:* Mach Contours of Designs 1,4 and 5 with different Web Wedge Lengths (*k*)

**Effects of Web Member Wedge Angle**

In this part, the designs numbered as 1,6 and 7 are used where the wedge angles are changed between 2° to 8°. Other parameters are kept constant in this part of the study. Hence, the profile is a modified-double wedge having a 30 percent flat region between the 35 percent leading and trailing wedges. Again, as wedge angle "$\gamma$" increased, the web total thickness and consequently frame thickness are increased as well. The aerodynamic coefficients obtained from the computational results are shown in Figure 12. Increasing the wedge angle increases the axial force coefficient, however, decreases the normal force and bending moment coefficients. In Figure 13, the Mach contours for corresponding designs are shown on a slice cutting the profiles and showing the flow through the grid fin. The Mach contours showed that in Design-7 with the highest wedge angle, the flow is chocked. Because of the flow choking, there is nearly 30% decrease in the normal force and bending moment coefficients. On the other hand, the axial force coefficient of Design-7 is about 4 times of the Design-6. Also, web and frame thicknesses of Design-7 are 4 times of the Design-6.

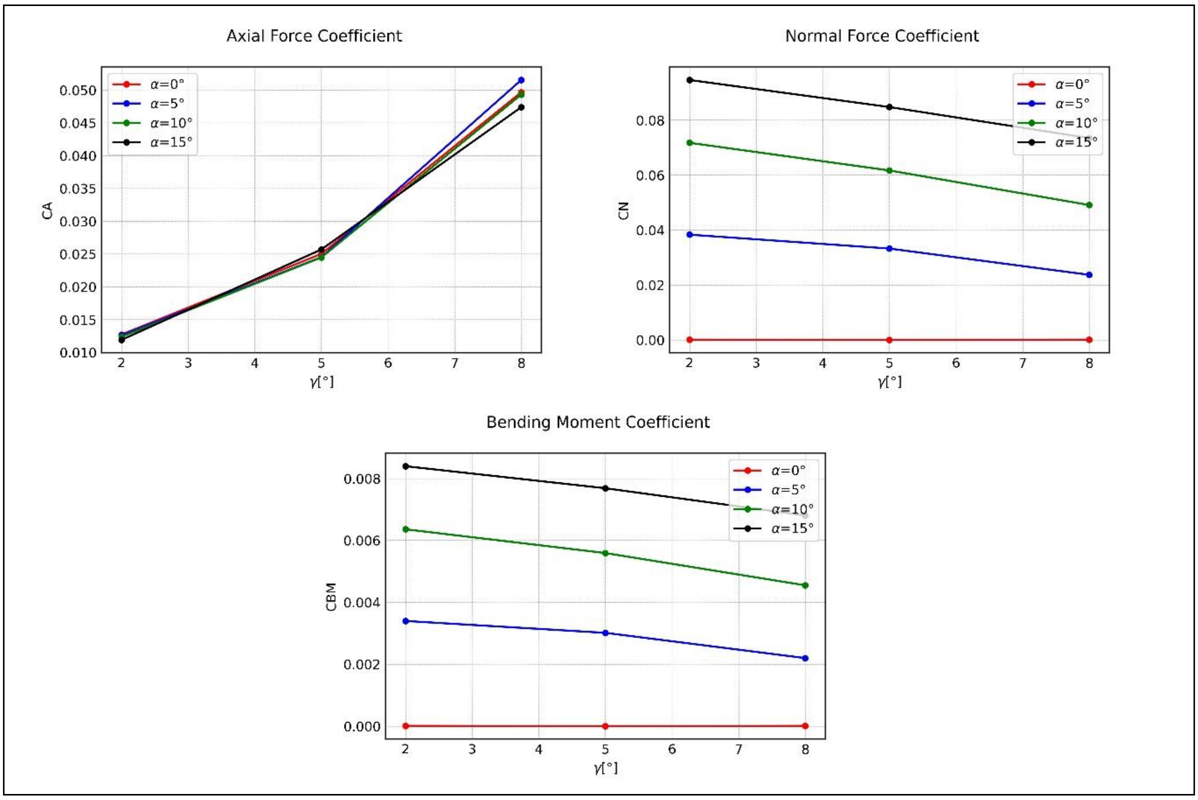


Figure 12: Aerodynamic Coefficients: Axial Force, Normal Force and Bending Moment Coefficients vs Web Wedge Angle ($\gamma$)

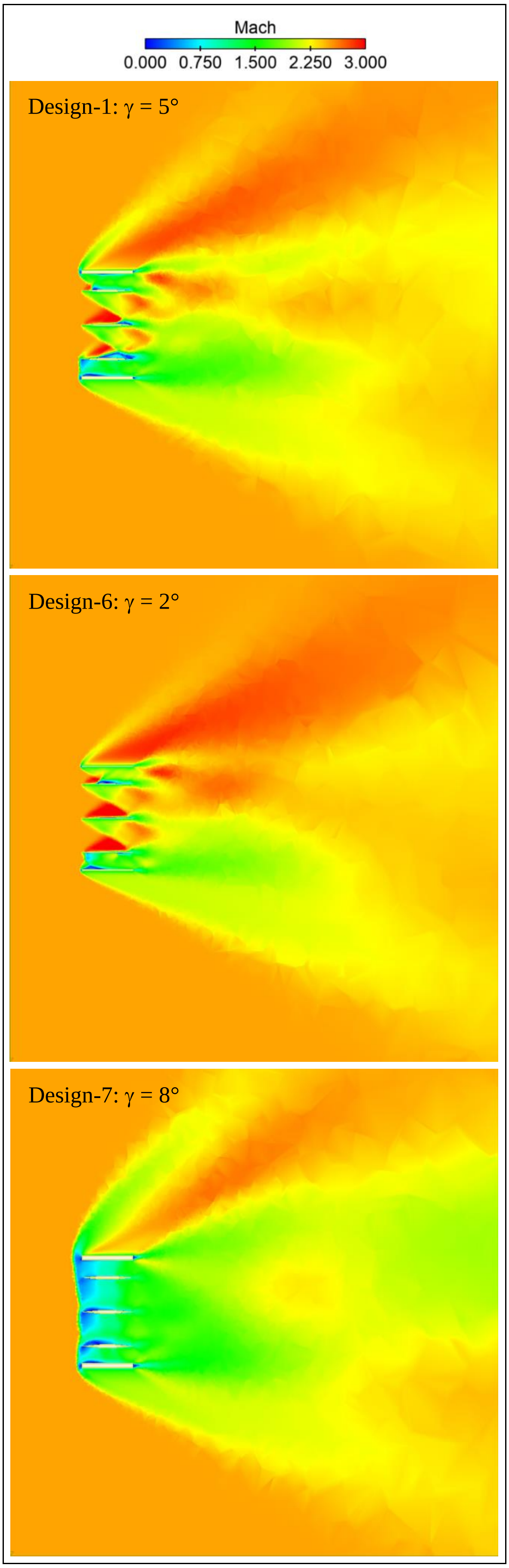


Figure 13*:* Mach Contours for Designs 1,6 and 7 with different Web Wedge Angle (γ)

## CONCLUSION

A parametric study on grid fins is done by using CFD with different parameters to investigate the effects of gap, web wedge length at the leading and trailing edges and wedge angle. For this purpose, CFD simulations for different grid fin geometries are performed for Mach number of 2.5 and four angles of attack 0° and 15° to investigate aerodynamic performance and flow field characteristics. A proper CFD simulation procedure is selected and described in terms of computational domain and suitable boundary conditions.

This study revealed that gap between web members has a crucial effect on the flow field and thus aerodynamic coefficients. The increasing gap may lead to avoiding flow chocking. However, since this increases spanwise length as well, the bending moments created by grid fin need to be tailored carefully.

Moreover, web profile is important when designing grid fins. As wedge parts of the profile at the leading and trailing edges are changed in terms of the wedge angle or wedge length, this highly affects the flow structure inside the grid cells and change the aerodynamic coefficients. Increasing the wedge angle as a design parameter as observed in this study, may lead to flow chocking, and highly increases the axial force coefficient of grid fin.

## References

Ansys Fluent 20.0 Users Guide, Ansys Inc.

Debiasi, M., Yan, Z., & Loon, C. T. (2010). *Swept-Back Grid Fins for Transonic Drag Reduction*. 28th AIAA Applied Aerodynamics Conference, July 2010, p: 1–17.

DeSpirito, J., Edge, H. L., Weinacht, P., Sahu, J., and Dinavhi, S. P. G. (2000). *CFD Analysis of Grid Gins for Maneuvering Missiles*. 38th Aerospace Sciences Meeting and Exhibit, January 2000.

Hughson, M. C., Blades, E. L., Luke, E. A., and Abate, G. L. (2007). *Analysis of Lattice Grid Tailfin Missiles in High-Speed Flow*. 25th AIAA Applied Aerodynamics Conference, June 2007, p: 572–586.

Miller, M. S., and Washington, W. D. (1994). *An Experimental Investigation of Grid Gin Drag Reduction Techniques*. AIAA 12th Applied Aerodynamics Conference, 1994, p: 800–808.

Munawar, S. (2010). *Analysis of Grid Fins as Efficient Control Surface in Comparison to Conventional Planar Fins*. 27th Congress of the International Council of the Aeronautical Sciences 2010, ICAS 2010, 3, 1732–1737

Peng, K., Hu, F., Wang, D., Okolo, P. N., Xiang, M., Bennett, G. J., and Zhang, W. (2018). *Grid Fins Shape Design of a Launch Vehicle Based on Sequential Approximation Optimization*. Advances in Space Research, Vol. 62(7), p: 1863–1878.

Rao, V. S., Viti, V., & Abanto, J. (2020). *CFD Simulations of Super/Hypersonic Missiles: Validation, Sensitivity Analysis, and Improved Design*. AIAA Scitech 2020 Forum, January 2020, p: 1–22.

Ravindra, K., Shende, N. V., & Balakrishnan, N. (2013). *CFD Simulation of the Grid Fin Flows*. 31st AIAA Applied Aerodynamics Conference, June, 24–27.

Theerthamalai, P., and Nagarathinam, M. (2006). *Aerodynamic Analysis of Grid-Fin Configurations*. Journal of Spacecraft and Rockets, Vol. 43(4), p: 750–756.